A major purpose of the Technical Information Center is to provide the broadest dissemination possible of information contained in DOE's Research and Development Reports to business, industry, the academic community, and federal, state and local governments.

Although a small portion of this report is not reproducible, it is being made available to expedite the availability of information on the research discussed herein.

1

LA-UR--83-3498

DE84 004335

Conf-8310229--1

Los Alamos National Laboratory is operated by the University of California for the United States Department of Energy under contract W-7405-ENG-36

TITLE: Implications of the 1100 UT March 22, 1979 CDAW 6 Substorm Event for the Role of Magnetic Reconnection in the Geomagnetic Tail

AUTHOR(S): T.A. Fritz, D.N. Baker, R.L. McPherron, and W. Lennartsson

SUBMITTED TO: Chapman Conference on Magnetic Reconnection, Los Alamos, NM, 3-7 October 1983

Los Alamos
Los Alamos National Laboratory
Los Alamos, New Mexico 87545

Implications of the 1100 UT March 22, 1979 CDAW 6 substorm event for the role of magnetic reconnection in the geomagnetic tail

by

T. A. Fritz[1], D. N. Baker[1], R. L. McPherron,[2] and W. Lennartsson[3]

Paper presented at the AGU Chapman Conference on Magnetic Reconnection

October 3-7, 1983

Los Alamos National Laboratory

Los Alamos, NM 87545

1. Earth and Space Sciences Division, Los Alamos National Laboratory Los Alamos, NM 87545
2. Institute of Geophysics and Planetary Physics, University of California, Los Angeles, CA 90024
3. Lockheed Palo Alto Research Laboratory, 3251 Hanover Street, Palo Alto, CA 94304

Abstract

The event of March 22, 1979 has been the object of a concentrated study effort as a part of the Coordinated Data Analysis Workshop activity designated CDAW-6. Energetic electron and magnetic field measurements from a set of four satellites aligned from 6.6 to 13 R_E at the 0200 LT meridian at the time of the magnetospheric substorm event of 1100 UT are presented. These data are used to show that a magnetic X-line formed spontaneously in the vicinity of 7 R_E in response to a steady build-up of magnetic stress in the geomagnetic tail.

Introduction

Since the introduction of the concept of an open magnetosphere by Dungey in 1961 with the requirement for magnetic field merging regions near the subsolar magnetopause and in the geomagnetic tail, the role of reconnection in the magnetospheric substorm process has been a topic of debate. Dungey (1961) argued that if there is reconnection at the subsolar magnetopause there must be reconnection in the magnetic tail and the rate at which reconnection occurs in these two regions must be equal on the average but need not balance instantaneously. When these rates fail to balance there is a net transport of magnetic flux into the geomagnetic tail (Russell and McPherron, 1973). This in turn leads to a build-up of magnetic stresses in the tail. Much evidence now exists which points to the formation of X- and O-type neutral lines that form as a result of magnetic reconnection. This process can occur spontaneously from a collisionless tearing mode instability under certain conditions (Galeev, 1982; Schindler, 1983, Cowley, 1983). Three-dimensional MHD modeling (Birn and Hones, 1981) has demonstrated that this newly formed reconnection region can form well earthward of the preexisting tail reconnection site required in Dungey's open model of the magnetosphere.

Although much evidence exists for the formation of a new region of reconnection in association with the magnetospheric substorm, a significant point to note is that little concensus exists as to the location of this new site; its location is discussed as occurring anywhere from a value of X(GSE) = $-15\ R_E$ to beyond X(GSE) $\approx -200\ R_E$. We present here data obtained by a set of four satellites in the near earth magnetotail during a well-studied substorm which indicate that the near earth neutral-line formed in the vicinity of the geostationary orbit ($r = 6.6\ R_E$). We also demonstrate that the formation of the region this close to the earth was able to draw appreciable quantities of ions from the ionosphere. This result indicates that the formation and movement of the X-line is only one phase of the magnetospheric substorm process, i.e., much longer term effects can be associated with the temporally limited X-line formation.

Data Presentation

On March 22, 1979 a propagating interplanetary shock front struck the magnetopause at 0826 UT and subsequently there developed moderate-to-strong storm activity (Dst(max) = -70nT). A series of three discrete substorms occurred following the SSC at 0826 UT. This period has been the object of a concentrated study effort as part of the Coordinated Data Analysis Workshop activity known as CDAW 6 (Manka and McPherron, 1983). We report here on observations obtained from a set of four satellites aligned along the 0200 LT meridian at the time of a large magnetospheric substorm occurring near 1100 UT. The location of these satellites is presented in Figure 1.

Energetic electron measurements made by satellite 1977-077 at the geostationary orbit are presented in Figure 2 (c.f. Baker et al., 198[illegible]). The fluxes of these electrons are constant prior to 1040 UT at which time they decrease sharply to near background levels. Approximately ten minutes later they increase sharply back to their pre-dropout levels and at 1104 UT undergo a second sharp increase. Although the satellite is located at the geographic equator it is at a magnetic latitude of $\sim 5^{\circ}$ and we interpret the electron flux dropout from 1042 to 1052 UT as an indication that the satellite moved through the trapping boundary into the high latitude tail lobe as a result of the geomagnetic field becoming highly stressed and tail-like due to the transfer of magnetic flux into the geomagnetic field.

The energetic electron measurements from spacecraft 1977-007 can be used to calculate the local magnetic field orientation in a self-consistent manner. Using a spherical harmonic analysis of the >30 keV electron distributions (cf., Baker et al., 1982) we have computed the field line inclination in a dipole meridional plane. This field inclination, which we call θ_B, is shown in the lower panel of Figure 2. A value of $\theta_B = 0^{\circ}$ would correspond to a magnetic field parallel to the dipole axis, while a value of $\theta_B \sim 90^{\circ}$ would correspond to a very taillike configuration with the magnetic field nearly parallel to the dipole equatorial plane. The data of Figure 2 show that prior to the substorm expansion onset θ_B (when calculable) reached values approaching 90° between ~1045 and ~1055 UT.

At the GOES-3 satellite, nearly colocated with satellite 1977-077 at synchronous orbit, onboard measurements of the magnetic field confirm this picture. In Figure 3 the measured V, D, and H components of the magnetic field at GOES-3 are presented where H is parallel to the earth's rotational axis, V is radially away from the earth, and D is positive eastward ($V \times D = H$) completing the right-handed system (Fritz and Neeley, 1982). Note the change in the V-component as it departs from its dipolar value of -25γ at ~1020 UT and steadily becomes more negative reaching a value of -110γ at 1052 UT. This again is direct indication of the tail-like development of field at the geostationary orbit due to the build-up of stresses during the period 1010 UT to 1052 UT - a phase described by McPherron (1972) as the substorm "growth" phase.

At 1052 UT as determined both by the reappearance of the energetic electrons at satellite 1977-007 and the sharp change in the magnetic field V-component at GOES-3, the magnetic field suddenly relaxed back toward a more dipolar configuration. The highest energy electron intensity variation is plotted in Figure 4 along with the GOES-3 V-component to illustrate the simultaneous recovery seen in these two measurements. In addition, an identical electron energy passband on the ISEE-1 satellite is presented and, surprisingly, this channel shows the same recovery at 1052 UT. This behavior probably is not an in situ energization of these electrons. Rather, we interpret this as an indication that these electrons were excluded from reaching either 1977-007 at 6.6 R_E (5° magnetic latitude) or ISEE-1 at 13 R_E. This exclusion would most likely be due to the highly stressed tail-like magnetic field configuration prior to 1052 UT, while the energetic electrons were later able to drift to each satellite location after the field reconfiguration at 1052 UT.

The three GSE components of the magnetic field measured at ISEE-1 for this time interval are presented in Figure 5. Note the steadily increasing value of the B_x component and total magnitude of the field from ~1035 UT to beyond 1100 UT. As demonstrated by Fairfield (1983) this increase of the magnetic field is further evidence for the enhanced transport of magnetic flux into the geomagn[illegible] and the resultant build-up of stresses there. The point to note in Figure 5 is that there is no evidence for a magnetic field reconfiguration at 1052 UT at ISEE-1 located at 13 R_E. In fact the first evidence of any particle acceleration at ISEE-1 associated with the magnetic field reconfiguration which occurred at GOES-3 and 1977-007 at 1052 UT was seven minutes later at 1059 UT (Fritz, et al., 1983; Paschmann et al., 1983). The direction of the observed plasma and energetic particle streaming at 13 R_E was such that the particle source was located earthward of the ISEE satellites.

The in situ measured densities of various ion species at ISEE-1 are presented in Figure 6 (Lennartsson et al., 1983). In the upper portion of the figure the measured density of ions associated with a solar wind source is plotted while in the lower panel ion densities associated with a putative ionospheric source are presented. Note that prior to the 1052 UT magnetospheric substorm onset (and the associated magnetic field reconfiguration at geostationary orbit) the plasma sheet at the ISEE-1 position was dominated by ions of solar wind origin (as indicated by the large density of He^{++} ions and low density of O^+ ions), whereas after the substorm the composition of the plasma sheet was dominated by ions of ionospheric origin (as indicated by the large density of O^+ ions and low density of He^{++} ions). This magnetospheric substorm was able to completely alter the composition of the plasma resident in the near-earth plasma sheet by switching from the usual solar wind source to an ionospheric source for the plasma to repopulate the plasma sheet during the substorm recovery.

Summary and Conclusions

The magnetospheric substorm of 1100 UT March 22, 1979 studied extensively as a part of the CDAW-6 activity, has demonstrated that a neutral line formed spontaneously just tailward of the geostationary orbit (e.g. ~7 R_E) following an extended period of increasing stress build-up in the tail magnetic field. The magnetic field reconfiguration associated with the formation of this reconnection region was not initially observed at ISEE-1 suggesting that the region was therefore localized well earthward of 13 R_E. The formation of the X-line and the eventual ejection of a plasmoid down the tail are apparently only the first manifestation of the magnetospheric substorm expansion process since appreciable fluxes of ions can be lifted out of the ionosphere, energized and used to reform the plasma sheet in association with the magnetospheric substorm process.

Acknowledgements

The CDAW-6 activity has extensively used the facilities of the National Space Science Data Center (NSSDC) at NASA/Goddard Space Flight Center and we thank Dr. James I. Vette and his organization for their efforts. Many other scientists have contributed their efforts to the interpretation of the CDAW-6 events and we acknowledge their collective contributions. We also wish to thank Dr. R. H. Manka for his extensive organizational efforts in making CDAW-6 the success it has become.

References

Baker, D. N., T. A. Fritz, B. Wilken, P. R. Higbie, S. M. Kaye, M. G. Kivelson, T. E. Moore, W. Stüdemann, A. J. Masley, P. H. Smith, and A. L. Vampola, "Observation and modeling of energetic particles at synchronous orbit on July 29, 1977," J. Geophys. Res., 87, 5917, 1982.

Birn, J. and E. W. Hones, Jr., "Three-dimensional computer modeling of dynamic reconnection in the geomagnetic tail," J. Geophys. Res., 86, 6802, 1981.

Cowley, S. W. H., "The distant geomagnetic tail in theory and observation," These Proceedings, 1983.

Dungey, J. W., "Interplanetary magnetic fields and the auroral zones," Phys. Rev. Lett., 6, 47, 1961.

Fairfield, D. H., "Solar wind control of magnetospheric pressure," J. Geophys. Res. (CDAW 6 results, in preparation), 1983.

Fritz, T. A. and C. Arthur Neeley, "Geostationary satellites ATS-6 and SMS/GOES: Description, position, and data availability during the IMS" in The IMS Source Book (C. Russell and D. Southwood, editors) AGU Press, Washington, D.C., 53, 1982.

Fritz, T. A. et al., "An energetic particle perspective of the 11 UT March 22, 1979 substorm: CDAW-6" J. Geophys. Res. (CDAW-6 results, in preparation), 1983.

Galeev, A. A., "Magnetospheric tail dynamics," in Magnetospheric Plasma Physics (A. Nishida, editor), D. Reidel, Dordrecht, 143, 1982.

Lennartsson, W., R. D. Sharp, and R. D. Zwickl, "Substorm effects on the plasma sheet composition during the CDAW-6 event," J. Geophys. Res. (CDAW-6 results, in preparation), 1983.

Manka, R. H. and R. L. McPherron, "Dynamics of the March 22, 1979 substorm event: CDAW-6," J. Geophys. Res. (CDAW-6 results, in preparation), 1983.

McPherron, R. L., "Substorm related changes in the geomagnetic tail: The growth phase" Planet. Space Sci., 20, 1521, 1972

Paschmann, G. et al., "Plasma measurements during the 11 UT substorm of March 22, 1979: CDAW-6," J. Geophys. Res., (CDAW-6 results, in preparation), 1983.

Russell, C. T. and R. L. McPherron, "The magnetotail and substorms," Space Sci. Rev., 15, 205, 1973.

Schindler, K., "Spontaneous Reconnection," These Proceedings, 1983.

FIGURE CAPTIONS

Figure 1. Location of seven spacecrafts during the CDAW-6 substorm of 11 UT on March 22, 1979. Note the radial alignment of four satellites along the 0200 LT meridian.

Figure 2. Energetic electron intensities measured by instruments on satellite 1977-007 during the CDAW-6 substorm of 11 UT on March 22, 1979. θ_B is described in the text.

Figure 3. Magnetic field measurements made by the magnetometer on satellite GOES-3 during the CDAW-6 substorm of 11 UT on March 22, 1979. See text for definition of V, D, and H components.

Figure 4. Composite plot of the GOES-3 magnetic field V-component and two similar electron energy channels on satellite 1977-007 at the geostationary orbit and satellite ISEE-1 at 13 R_E.

Figure 5. Magnetic field measurements in GSE coordinates made by the magnetometer on satellite ISEE-1 during the CDAW-6 substorm of 11 UT on March 22, 1979.

Figure 6. In situ measurements of the ionic compositional densities in the plasma sheet at the location of satellite ISEE-1 during the CDAW-6 event interval on March 22, 1979 (from Lennartsson et al., 1983).

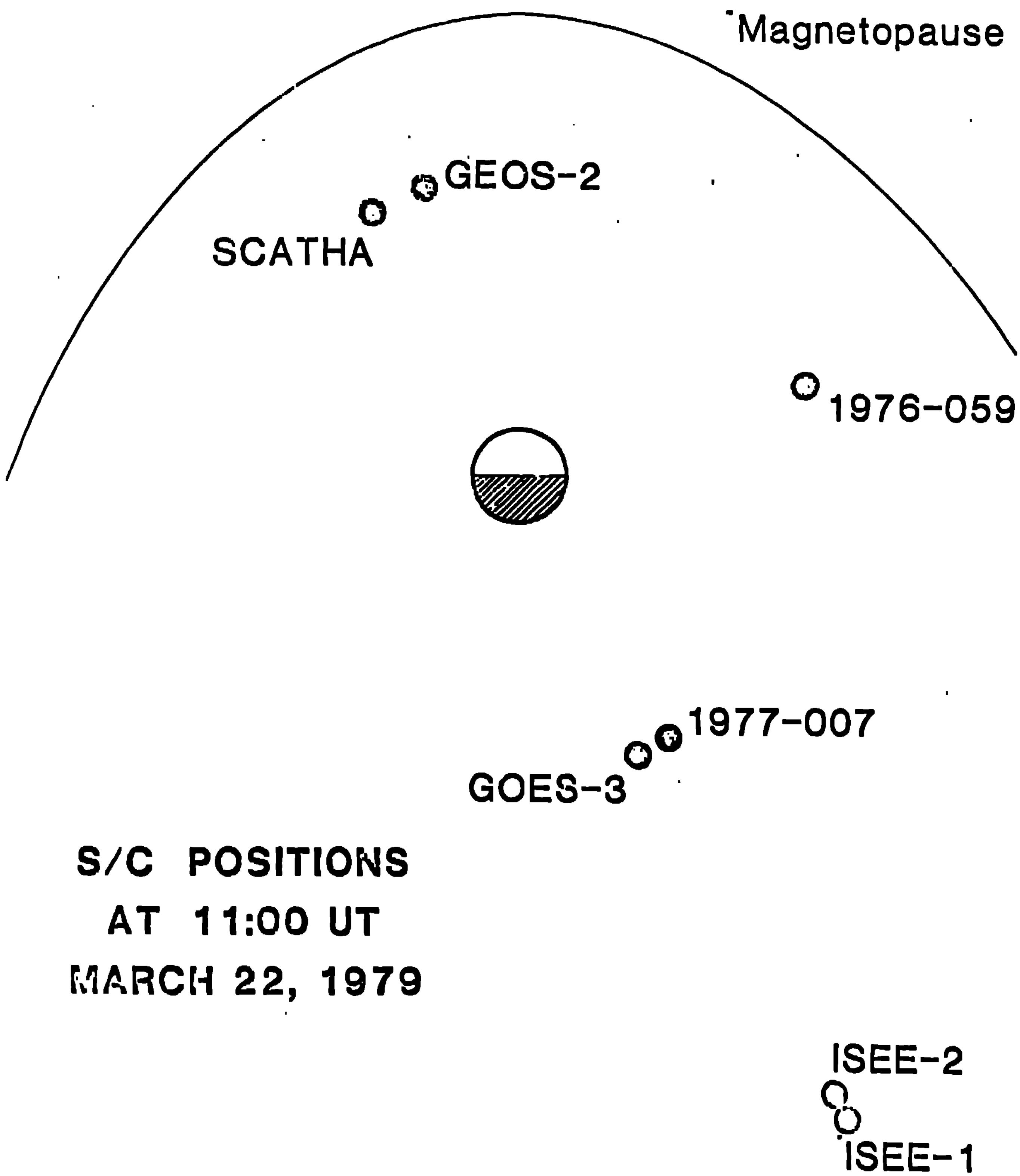
Magnetopause
GEOS-2
SCATHA
1976-059
1977-007
GOES-3
S/C POSITIONS
AT 11:00 UT
MARCH 22, 1979
ISEE-2
ISEE-1

Figure 1

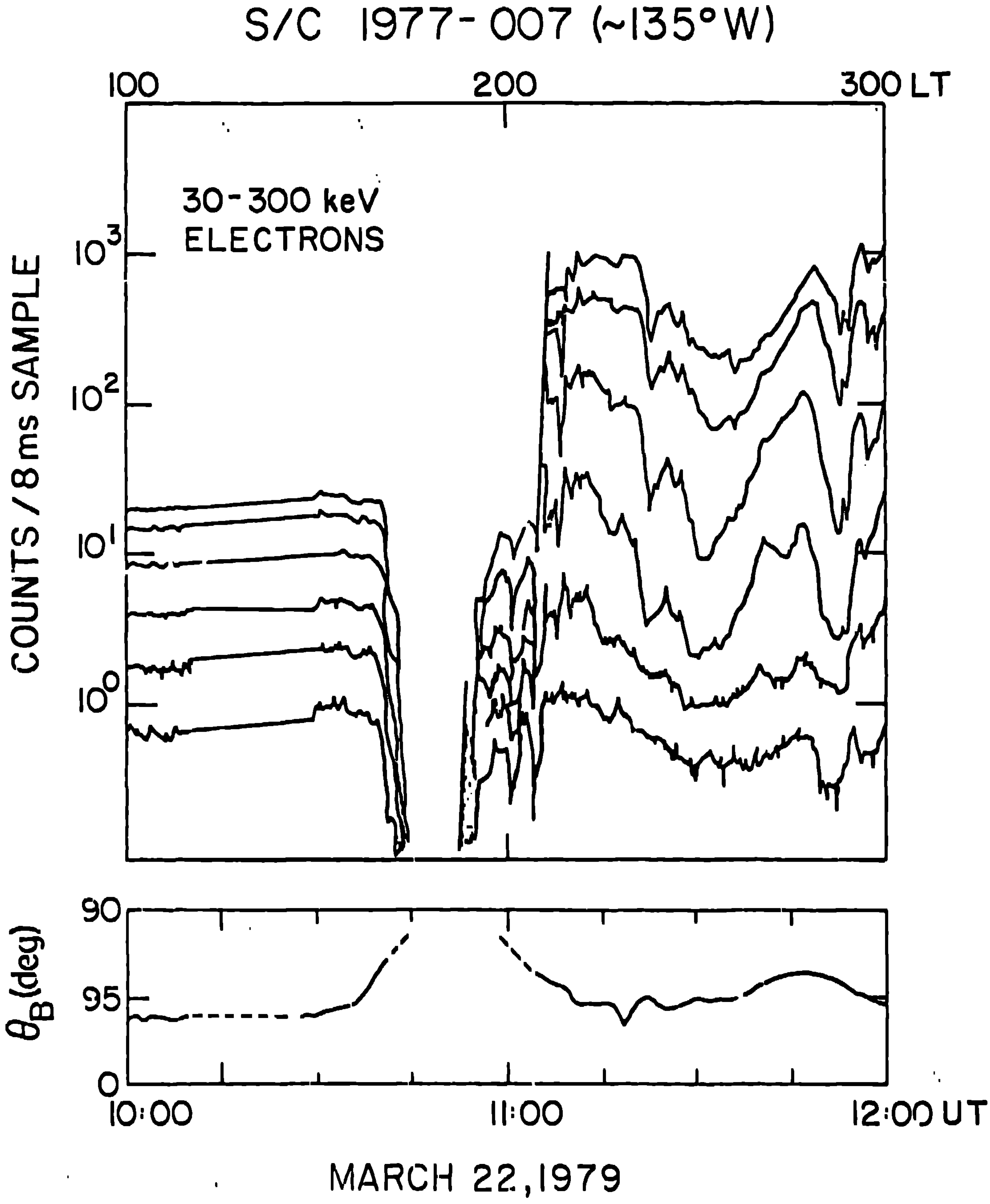

S/C 1977-007 (~135° W)
100
200
300 LT
30-300 keV
ELECTRONS
COUNTS / 8 ms SAMPLE
10³
10²
10¹
10⁰
90
95
0
θB (deg)
10:00
11:00
12:00 UT
MARCH 22, 1979

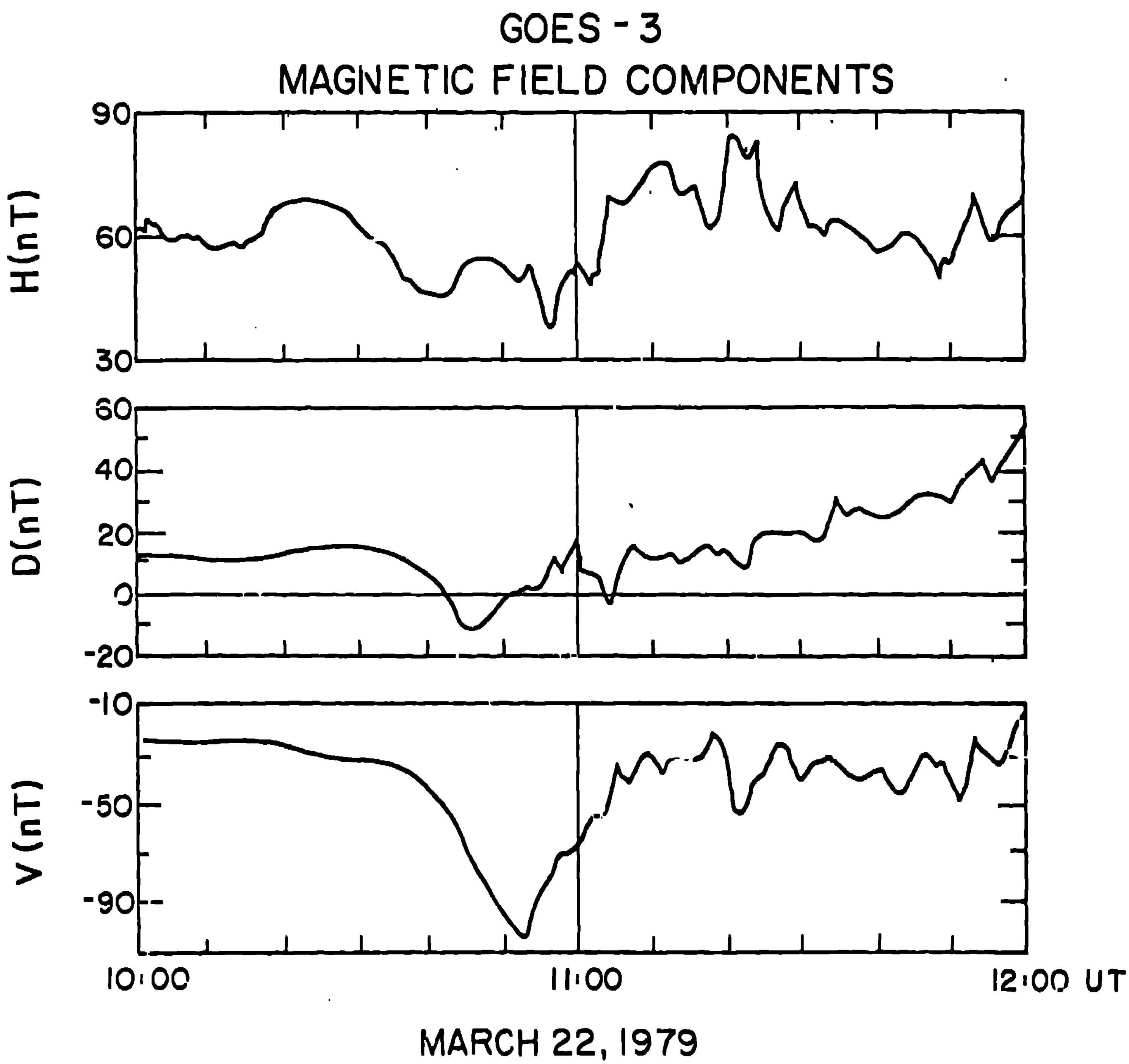
GOES - 3
MAGNETIC FIELD COMPONENTS
H(nT)
90
60
30
D(nT)
60
40
20
0
-20
V(nT)
-10
-50
-90
10:00
11:00
12:00 UT
MARCH 22, 1979

Figure ?

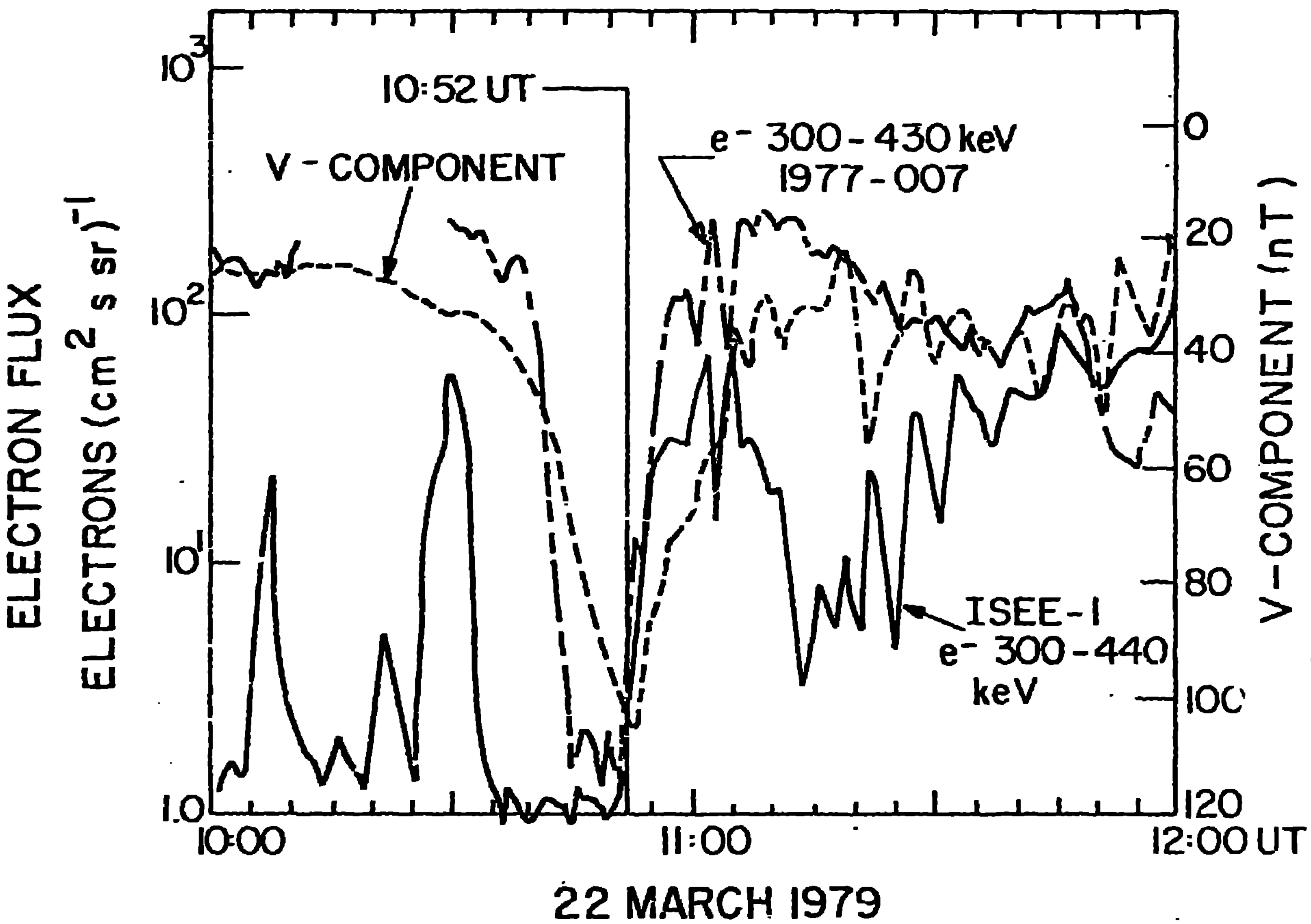
10:52 UT
V - COMPONENT
e⁻ 300 - 430 keV
1977 - 007
ISEE - I
e⁻ 300 - 440
keV
ELECTRON FLUX
ELECTRONS (cm² s sr)⁻¹
V-COMPONENT (nT)
10³
10²
10¹
1.0
0
20
40
60
80
100
120
10:00
11:00
12:00 UT
22 MARCH 1979

Figure 4

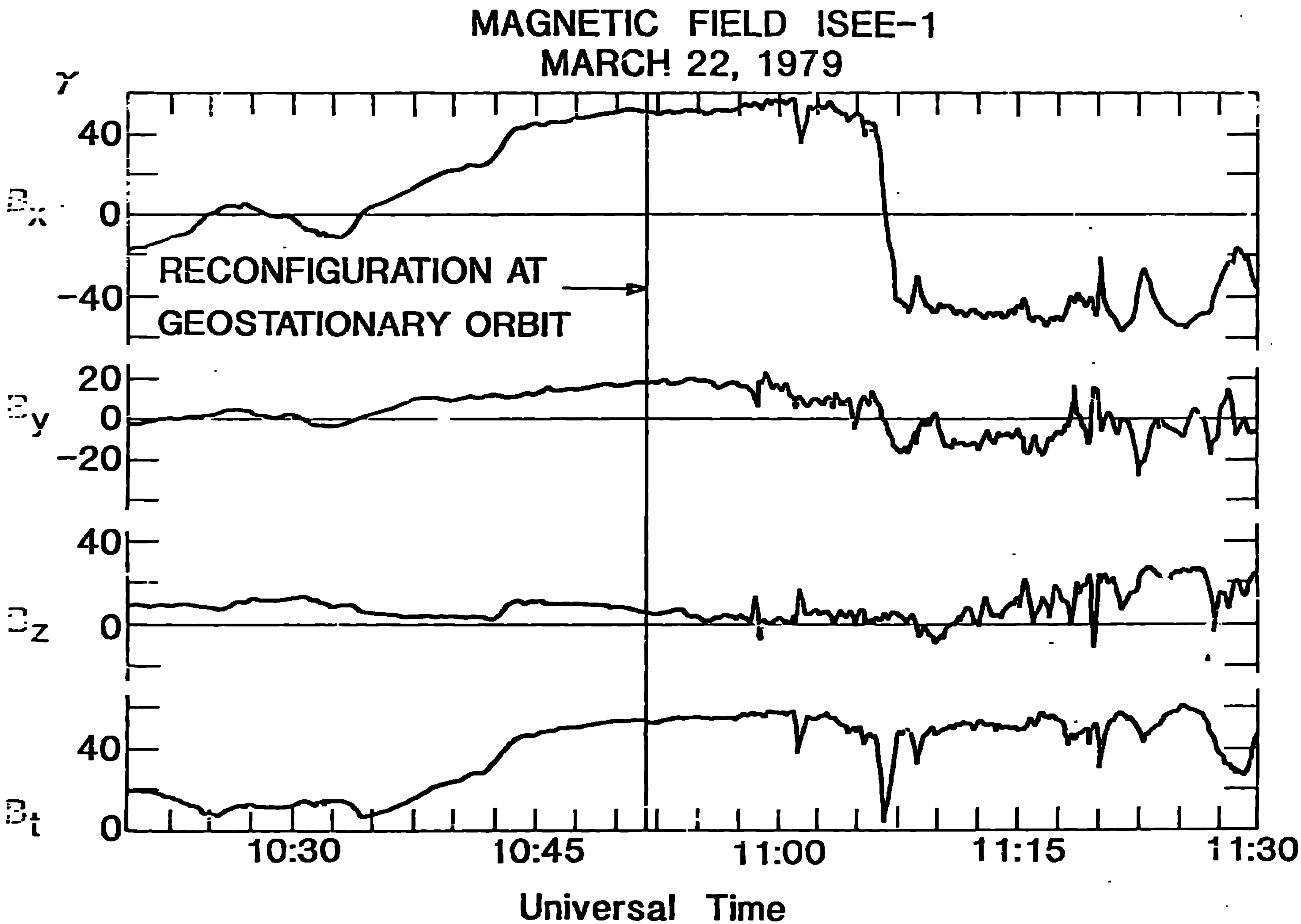

MAGNETIC FIELD ISEE-1
MARCH 22, 1979
γ
40
0
−40
B_x
RECONFIGURATION AT
GEOSTATIONARY ORBIT
20
0
−20
B_y
40
0
B_z
40
0
B_t
10:30
10:45
11:00
11:15
11:30
Universal Time

Figure 5

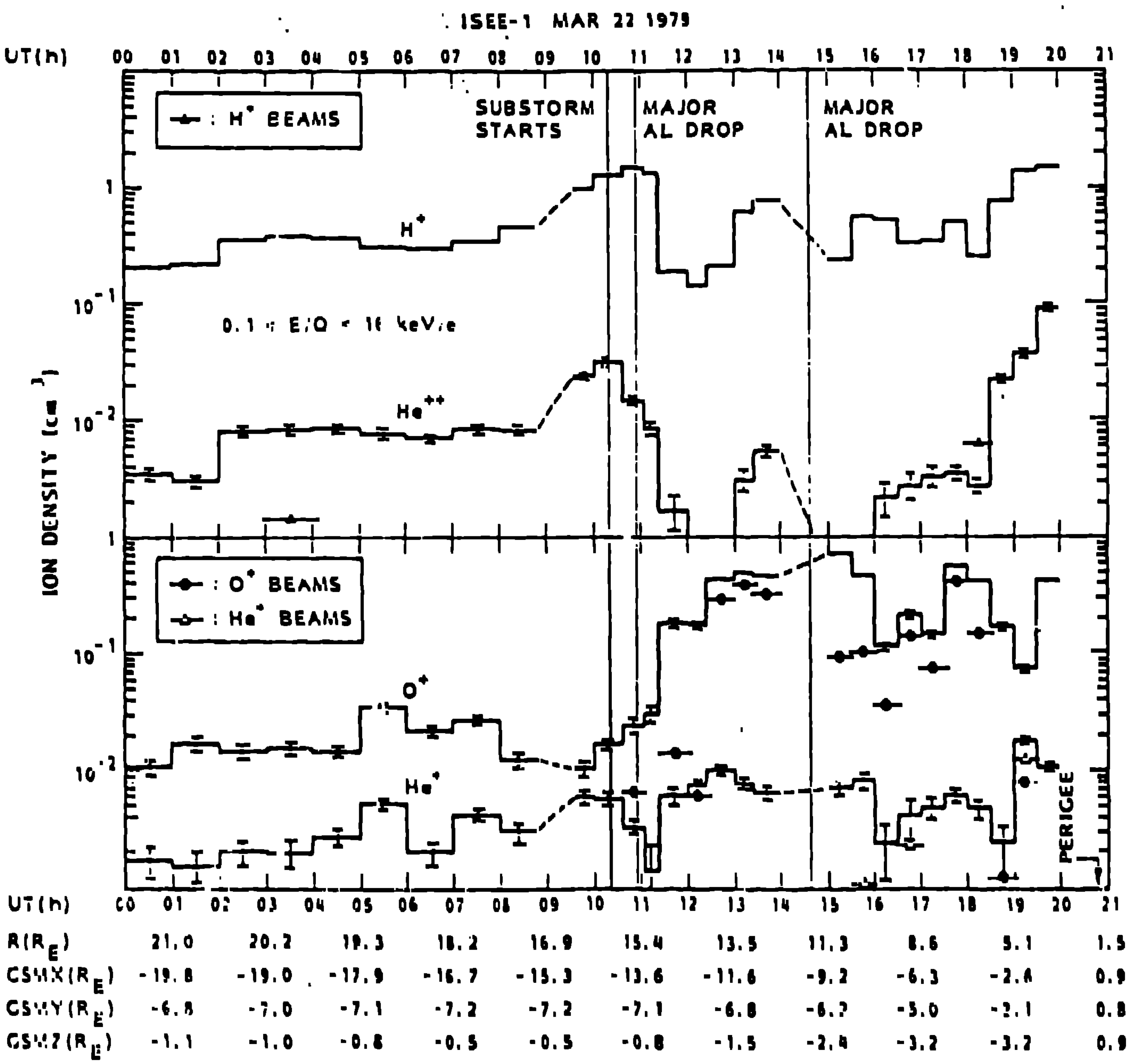
ISEE-1 MAR 22 1979
UT(h)
H+ BEAMS
SUBSTORM STARTS
MAJOR AL DROP
MAJOR AL DROP
H+
He++
ION DENSITY (cm-3)
O+ BEAMS
He+ BEAMS
O+
He+
PERIGEE
R(RE) 21.0 20.2 19.3 18.2 16.9 15.4 13.5 11.3 8.6 5.1 1.5
CSMX(RE) -19.8 -19.0 -17.9 -16.7 -15.3 -13.6 -11.6 -9.2 -6.3 -2.4 0.9
CSMY(RE) -6.8 -7.0 -7.1 -7.2 -7.2 -7.1 -6.8 -6.? -5.0 -2.1 0.8
CSMZ(RE) -1.1 -1.0 -0.8 -0.5 -0.5 -0.8 -1.5 -2.4 -3.2 -3.2 0.9

Figure 6